rated than previously estimated. For example, the ammonia profile of Carlson *et al.* (*13*) decreases by a factor of 10 from 2 bars to 1 bar, whereas our fitted profile decreases by more than a factor of 20 between 3 bars and 1 bar, and decreases by another factor of 4 between 1 and 0.5 bars, where their profile is constant. It remains to be determined whether we can find an opacity structure that is not only consistent with NFR observations but also satisfies other constraints derived from recent ground-based or past Voyager observations of hot spots.

REFERENCES AND NOTES

1. G. S. Orton *et al.*, *Science* **272**, 839 (1996).
2. L. A. Sromovsky, J. Hayden, F. A. Best, H. E. Revercomb, *Space Sci. Rev.* **60**, 233 (1992).
3. R. E. Young, M. A. Smith, C. K. Sobeck, *Science* **272**, 837 (1996).
4. Prelaunch calibrations are described in (*2*) and in more detail by L. A. Sromovsky and P. M. Fry [in *Proceedings of The Fourth Infrared Sensor Calibration Symposium*, 9 to 12 May 1994, Space Dynamics Laboratory, Utah State Univ., Logan, UT (1994).
5. The detector heating and cooling is modulated by the rotation of the optics (including the detector package) between upward and downward views, exposing the detector package to convective transfer rates that vary with orientation at the chopping frequency, and thus can produce a very small temperature modulation in the pyroelectric detectors at the same frequency as the desired temperature modulations produced by the chopped radiation signal.
6. Detector-to-detector variations are currently not well understood and are the subject of laboratory tests of the spare instrument.
7. For each solar channel, we multiplied the blind channel correction by a factor that produced net fluxes approaching zero toward sunset (about 15 bars). For channel D, we required that the net flux at 10 bars be in the range of 0 to 0.3 W m^{-2}, the upper bound being the maximum possible flux computed for a model in which only hydrogen absorption is present. For channel C we used a model-independent requirement that the measured fluxes be positive at all altitudes, and we obtained slightly tighter constraints by also requiring that (when averaged over noise) channel C fluxes decrease with height above the 3-bar level. The correction of the broadband thermal channel (A) was guided by model calculations showing that net fluxes in the 3- to 10-bar region were dominated by the 5-μm fluxes, with most of the remainder coming from the hydrogen-dominated region sampled by channel D. But because of differences in relative spectral response functions, the model results indicate that channel C and channel A should be about equal in the 8- to 10-bar region. Thus, we selected the channel A correction factor to minimize its average difference with channel C deeper than about 8 bars. We determined the following extraneous response correction factors: channel A, 1.4 $\pm$ 0.1; channel B, 0.75 $\pm$ 0.1; channel C, 4.0 $\pm$ 0.2; channel D, 2.1 $\pm$ 0.05; and channel E, 1.3 $\pm$ 0.05. These are the factors by which the channel F detector–level output needs to be multiplied before being subtracted from the other channels to correct for their extraneous response signals. The uncertainties for channels B, C, D, and E arise mainly from noise in the profiles in regions where the constraints are applied. The relatively large correction required for channel C is not understood and suggests that a very localized heat transfer near the detector package itself is needed to introduce such a difference in temperature variation amplitudes.
8. The probe spin rate appears to be a relatively constant 33.5 (+2.6/−2.4) rpm down to at least the 1-bar level (L. J. Lanzerotti and K. Rinnaert, personal communication). The mean azimuthal position of a 6-s sampling interval would thus change ~126° (+93°/−80°) between samples, implying that a sample facing the sun would be surrounded by samples facing away from the sun, leading to a modulation of amplitude that depends on the initial azimuth.
9. R. A. West, D. F. Strobel, M. G. Tomasko, *Icarus* **65**, 161 (1986).
10. B. Ragent, D. S. Colburn, P. Avrin, K. A. Rages, *Science* **272**, 855 (1996).
11. If the NH_3 cloud layer were composed of broken clouds above the probe, or if the probe were in a clear region within the cloud layer, the heating in channel A and the effects of direct solar beam attenuation in channels B and E could still be seen by the NFR, which observes radiation from distances of many kilometers. On the other hand, the nephelometer, which samples only the immediate vicinity of the probe, would see nothing.
12. L. P. Giver, M. G. Tomasko, D. Kerola, D. C. Benner, *Bull. Am. Astron. Soc.* **21**, 947 (1989); E. Karkoschka, *Icarus* **111**, 174 (1994).
13. B. E. Carlson, A. C. Lacis, W. B. Rossow, *J. Geophys. Res.* **98**, 5251 (1993).
14. Solar mixing ratios, expressed as number densities relative to H_2, are taken to be 1.7×10^{-3} for H_2O, 7.2×10^{-4} for CH_4, and 2.2×10^{-4} for NH_3, following E. Anders and N. Grevesse [*Geochim. Cosmochim. Acta* **53**, 197 (1989)].
15. The current best estimate for the jovian deep NH_3 abundance is 1.3 $\pm$ (0.1 to 0.2) times the solar abundance, on the basis of analysis of microwave observations by I. De Pater and D. L. Mitchell [*J. Geophys. Res. Planets* **98**, 5471 (1993)].
16. H. B. Niemann *et al.*, *Science* **272**, 846 (1996).
17. A. Seiff *et al.*, *Science* **272**, 844 (1996).

18. Special recognition is due to R. W. Boese, the original NFR principal investigator from Ames Research Center (ARC), who died in 1985, and J. Pollack, a key NFR co-investigator, who died in June 1994. We thank R. Twarowski and B. Chin from ARC for valuable project support; the following M. Marietta personnel involved in the NFR development: D. Shumaker, T. Knight, R. Amundsen, T. Hopkins, S. Shertz, and B. Cunningham; P. Smith and L. Doose from the University of Arizona, who supported the NFR calibration; D. Thielman, J. Vian, S. Ellington, J. Sitzman, and M. Dean, who provided support at the University of Wisconsin; the Galileo Project, and W. J. O'Neil in particular, for providing support and guidance; B. Carlson of the Goddard Institute for Space Studies for help in checking our radiative transfer model calculations; and an anonymous reviewer for helpful comments on the original draft. During the postlaunch period, the University of Wisconsin effort was supported by NASA grant NCC2-854.

4 March 1996; accepted 17 April 1996

Results of the Galileo Probe Nephelometer Experiment

Boris Ragent,* David S. Colburn, Philip Avrin, Kathy A. Rages

The nephelometer experiment carried on the Galileo probe was designed to measure the jovian cloud structure and its microphysical characteristics from entry down to atmospheric pressure levels greater than 10 bars. Before this mission there was no direct evidence for the existence of the clouds below the uppermost cloud layer, and only theoretical models derived from remote sensing observations were available for describing such clouds. Only one significant cloud structure with a base at about 1.55 bars was found along the probe descent trajectory below an ambient pressure of about 0.4 bar, although many indications of small densities of particle concentrations were noted during much of the descent.

The objective of the nephelometer experiment (*1*) aboard the Galileo probe (*2, 3*) is to explore the vertical structure and microphysical properties of the clouds and hazes of the jovian atmosphere. The instrument measured the scattering of an incident light beam from defined volumes in the atmosphere near the probe at five angles, four at forward scattering angles and one in a backscattering direction. An arm containing reflective mirror optics was successfully deployed shortly after the heat shield and aeroshell were removed. The instrument functioned and data were recorded from an altitude of about 20 km (~0.4 bar) above the 1-bar pressure reference altitude down to an altitude of about −140 km (~22 bars) (*4*). Data were obtained over the entire probe reporting period, but the instrument began to exhibit erratic behavior after about 40 min (~13 bars) of descent and began to fail, presumably because of the extreme operating conditions (*5*).

After the probe entered the atmosphere and decelerated, the nephelometer experiment was turned on about 13 s before the heat shield separated from the probe. About 2 s after heat shield separation, squibs freeing the nephelometer mirror arm were fired, commencing measurement of the ambient jovian atmosphere. Since the first measurements were affected by all these events, the first viable atmospheric data were obtained about 19.7 s after the instrument was turned on, corresponding to an ambient atmospheric pressure and temperature of ~0.4 bar and 129 K. Data were obtained for the next 57 min. However, because the instrument deteriorated in the hot internal probe environment near the end of descent, valid data may have been obtained only for the

B. Ragent and D. S. Colburn, San Jose State University Foundation, San Jose, CA 95172–0130, USA.
P. Avrin, Aerospace Corporation, Colorado Springs, CO 80912, USA.
K. A. Rages, Space Physics Research Institute, Sunnyvale, CA 94087–1315, USA.

*To whom correspondence should be addressed.

first 35 to 40 min of descent, corresponding to an ambient pressure of ~10 to 13 bars.

Curves of the raw data recorded for the five scattering angle channels during descent, as a function of ambient atmospheric pressure, are shown in Fig. 1. In the first 90 to 100 s (to ~0.6 bar) of descent, only small particle concentrations and a decrease in particle concentration with descent were encountered. This is the region where all of our previous considerations had led us to believe that we would encounter an ammonia cloud. Thus, it appears that, as evidence of this cloud may have been confirmed by another experiment aboard the probe (*6*), the ammonia cloud was inhomogeneous and very tenuous in the near vicinity of the probe. Or, possibly, it lay primarily above our altitude of deployment, and we only sampled the very small remnant of the lower portion of this cloud.

About 100 s (~0.63 bar) after the instrument was turned on, the signals began rising, and after about 118 s (~0.69 bar) a small but distinctive cloud structure was encountered. This structure, exhibiting apparent internal layering, persisted for about 210 s of descent, decreasing sharply into the ambient signal level at a pressure of ~1.5 to 1.6 bars (nominally at 1.55 bars). The magnitudes of the signals we received in the five light scattering channels of our instrument indicated that the cloud was not very dense, roughly comparable to a light, fairly transparent Earth cloud with a visibility of more than 1 km. There is some evidence from our diagnostic measurements of instrument conditions that some of the optical surfaces of the instrument may have been partially coated when the nephelometer passed through this cloud structure, and that the coating subsequently disappeared over the next 500 s of descent. Such a coating may affect the detailed comparison of signals in each of the scattering channels, but it in no way influences the observed location and description of the vertical structure of the cloud in this region. We estimate the approximate vertical extent of this cloud to be 5 to 10 km.

The composition of the particles forming this cloud is uncertain. At these pressure levels, equilibrium thermochemical calculations with solar abundance elemental concentrations predict the existence of condensed species such as ammonium hydrosulfide (NH_4SH) complexes composed of ammonia and sulfur compounds such as hydrogen sulfide (*7*). Results of species abundance measurements from the probe mass spectrometer experiment (*8*) indicate that the concentrations of ammonia and sulfur are sufficient to produce the tenuous structure we observed (*9*). The only other evident possibility is that we are seeing a feeble water cloud; however, the temperature, ~−90°C at the base of the observed structure, is so low that it is not plausible that there would be sufficient vapor pressure to support the formation of a water cloud with sufficient characteristics to produce the responses we observed at this pressure. We have tentatively assumed that this cloud is composed of some ammonia-sulfur compound. It should also be noted that severe atmospheric motion, involving strong vertical winds, for example, may produce particle spatial distributions very different from those predicted from stable equilibrium analyses.

A very thin cloud layer, no thicker than ~0.5 km, was evident at 418 s (~1.9 bars). It appears to be considerably less dense than the cloud directly above and is quite probably a detached portion of that cloud. Directly below this cloud, and extending to a descent time of about 1100 s at a pressure level of ~4.7 bars, the nephelometer measured very small particle concentrations in what may be a coherent structure. We are certain of the existence of very small-scale structural features in these signals, but these may be characteristic of very small collections of particles moving about in a complicated dynamic atmosphere. It should be emphasized, however, that the signals in this region are factors of 10 to 100 times smaller than those encountered in the relatively weak cloud structure above it, and that these small signals make it difficult to define any organized structure.

From 1100 s (~4.7 bars) down to 2100 s (~11 bars), and perhaps to beyond 2300 s (~12.5 bars), there were a number of correlations of signals in several pairs of the measuring channels of the nephelometer, indicating the presence of particles. However, these signals were extremely small (in some cases the signal-to-noise ratios were about 1) and except for denoting their presence, it is doubtful that much quantitative analysis of their properties obtained by considering the scattering cross sections derived from the signals in each channel will be possible.

From about 1500 s (~7 bars) after the instrument was activated, the baseline of each of the channels began to drift negatively until 2000 s (~10 bars), after which the baseline rose until about 2400 s (~13 bars) and then behaved very unusually from this point to the time of the last data we received at about 3500 s (>22 bars). Monitors of the output of the forward- and backward-scatter laser diode sources, and of the light-emitting diode light source used for the mirror alignment and contamination measurements, indicated that the sources appear to have functioned well out to about 2000 to 2500 s.

The nephelometer did not record any large signals indicative of a major water cloud structure at any point during descent of the probe (*10*). It is not believed, at present, that such a cloud structure, if it existed along the entry trajectory, had significant mass or opacity. Analyses of data from the Voyager mission have suggested the possibility of spatial inhomogeneities in such cloud structures located in hot spots (*11*). The apparent lack of the presence of a major water cloud, the existence of a tenuous cloud at a level in agreement with that predicted for the ammonium hydrosulfide

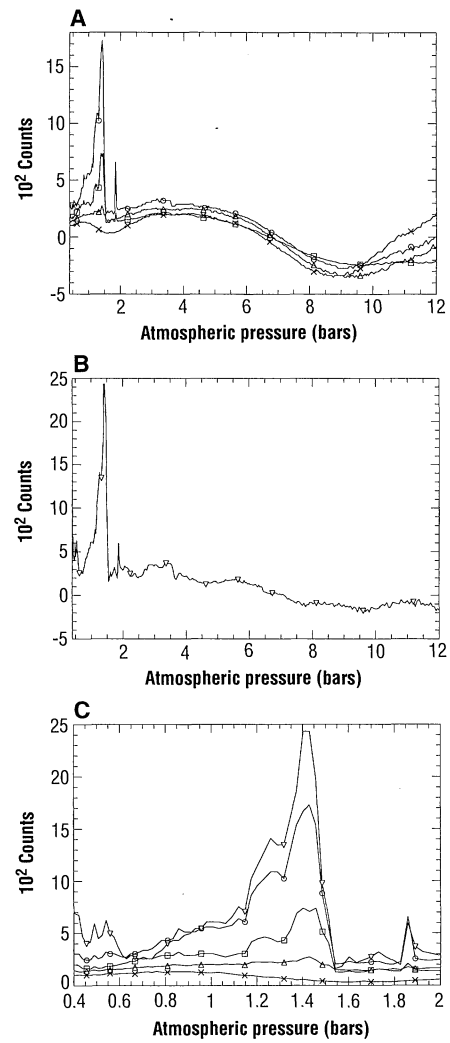

Fig. 1. (**A**) Variation of raw data counts from the four forward-scatter scattering angle channels (5.8°, circles; 16°, squares; 40°, triangles; and 70°, crosses) with ambient atmospheric pressure along the probe's descent trajectory. Negative values of the raw data counts are associated with baseline offsets primarily caused by instrument temperature variation during descent. (**B**) Variation of the 178° backward scattering channel raw data counts with ambient atmospheric pressure along the descent trajectory. (**C**) Expanded version of the variation of the all-channels raw data counts with ambient atmospheric pressure from ~0.4 to 2.0 bars along the Galileo probe descent trajectory. Symbols as in (A) and (B).

cloud, and the possible high altitude or inhomogeneity of an ammonia cloud are important and indicative of the extreme variability of the jovian atmosphere.

REFERENCES AND NOTES

1. B. Ragent *et al.*, *Space Sci. Rev.* **60**, 179 (1992).
2. T. V. Johnson *et al.*, *ibid.*, p. 3.
3. W. J. O'Neill and R. T. Mitchell, in *Proceedings of the AIAA 21st Aerospace Sciences Meeting*, Reno, NV, 10 to 13 January 1983 (American Institute of Aeronautics and Astronautics, New York, 1983), pp. 1–10; J. J. Givens *et al.*, *ibid.*, pp. 1–18.
4. A. Seiff *et al.*, *Science* **272**, 844 (1996). All atmospheric pressure, temperature, and altitude information were obtained from this reference.
5. During descent in the jovian atmosphere, the range of temperatures experienced by the instrument mounted in the probe extended from about −50°C to over 100°C. Rates of temperature excursions were as large as 6°C per minute. This temperature behavior has complicated the interpretation of the data, but the instrument functioned properly down to at least the 10-bar level.
6. L. A. Sromovsky *et al.*, *Science* **272**, 851 (1996).
7. S. J. Weidenschilling and J. W. Lewis, *Icarus* **61**, 311 (1973); S. K. Atreya and P. N. Romani, in *Photochemistry and Clouds of Jupiter, Saturn and Uranus in Recent Advances in Planetary Meteorology*, G. Hunt, Ed. (Cambridge Univ. Press, Cambridge, 1985), pp. 17–68.
8. H. B. Niemann *et al.*, *Science* **272**, 846 (1996).
9. Using techniques similar to those used by M. Ya Marov *et al.* [*Icarus* **44**, 608 (1980)], we have derived scattering cross sections from the raw data of Fig. 1 for the cloud at 1.4 bars. We assumed that the particle density immediately below the cloud base is zero and that the signals in the cloud larger than that at the base are due to cloud particles, and we included temperature-dependent corrections for baseline offsets and channel sensitivities. Large errors due to out-of-range corrections may be present in these data. We have compared these cross sections with those calculated for conservative scattering from model particle size distributions to obtain best fit values for the model parameters. A typical set of derived cloud property values obtained at this location, by using a log normal particle size distribution and the data described above and assuming a particle mass density of 1.0, are characteristic radius, r_m = 4.5 μm; characteristic width parameter, $\sigma = 1.5$; particle number density, $N = 2.5 \times 10^6$ m^{-3}; local particle mass loading mass density, $\rho = 9.5 \times 10^{-7}$ kg m^{-3}; scattering optical depth, $\tau \cong 2.6$; columnar particle loading, $N_0 = 1.4 \times 10^{10}$ m^{-2}; and columnar mass loading, $W_0 = 5.3 \times 10^{-3}$ kg m^{-2}. We emphasize that the values quoted here, although not inconsistent with values derived from earlier analyses of Voyager mission data (*11*), may be subject to major revision and should only be taken as illustrative of the analytical process results until full consideration of corrections for the instrumental temperature profiles, optical surface coatings, or other effects not yet fully analyzed have been completed.
10. Observations of thermal emission from the entry site with Earth-based telescopes [G. Orton *et al.*, *Science* **272**, 839 (1996)] characterized the probe entry site as being within and near the edge of a 5-μm "hot spot" (an area observable at a wavelength of 5 μm), a region considerably brighter than its surroundings, indicating that particles or absorbing gases are reduced in concentration in this region.
11. B. E. Carlson *et al.*, *J. Geophys. Res.* **98**, 5251 (1993).
12. We acknowledge the extensive contributions of our deceased co-investigator, colleague, and friend, James B. Pollack. We are grateful for the dedicated efforts of many of the members of the staff of the Martin-Marietta Aerospace Division, Denver, CO, and of the Galileo Probe Project Office and the Electronic Instrument Development Branch of NASA Ames Research Center for the design, construction, testing, and calibration of the Galileo probe nephelometers and for the successful mission activities. We also wish to thank the following people at NASA Ames Research Center: M. Smith, C. Sobeck, P. Melia, M. Izadi, B. Chin, and E. Tischler of the Galileo Probe Project Office, L. Colin, retired chief of the Space Sciences Division, and G. Deboo and W. Gunter, of the Electronic Instrument Development Branch. Thanks also to T. Knight, J. Martin, J. Waring, and C. Carlston of the Martin-Marietta Aerospace Division. Supported under NASA cooperative research agreement NCC 2-466 and NASA contract NAS 2-10015.

4 March 1996; accepted 17 April 1996

High-Energy Charged Particles in the Innermost Jovian Magnetosphere

H. M. Fischer, E. Pehlke, G. Wibberenz, L. J. Lanzerotti, J. D. Mihalov

The energetic particles investigation carried by the Galileo probe measured the energy and angular distributions of the high-energy particles from near the orbit of Io to probe entry into the jovian atmosphere. Jupiter's inner radiation region had extremely large fluxes of energetic electrons and protons; intensities peaked at $\sim 2.2R_J$ (where R_J is the radius of Jupiter). Absorption of the measured particles was found near the outer edge of the bright dust ring. The instrument measured intense fluxes of high-energy helium ions ($\sim$62 megaelectron volts per nucleon) that peaked at $\sim 1.5R_J$ inside the bright dust ring. The abundances of all particle species decreased sharply at $\sim 1.35R_J$; this decrease defines the innermost edge of the equatorial jovian radiation.

More than four decades ago, Burke and Franklin discovered that Jupiter emitted radio waves (*1*). Much of the nonthermal, synchrotron radiation from Jupiter originates from high-energy electrons that are trapped by the magnetic field relatively close to the planet. Of the flybys of the planet by the Pioneer 10 and 11, Voyager 1 and 2, and Ulysses spacecraft, only Pioneer 11 entered into the intense radiation region at distances close enough to the planet ($1.6R_J$) to obtain measurements of particles that could be major contributors to the nonthermal radio emissions (*2*). The Galileo probe, carrying the energetic particle instrument (EPI) through the jovian magnetosphere (*3*), provided the first measurements of the innermost regions of Jupiter's radiation environment.

The EPI instrument operated during the pre-entry phase of the mission, when the probe's heat shield still protected the descent module. Thus, the measured particles had to have energies high enough to penetrate the heat shield in order to be measured by the instrument. Three data samples were acquired near the equatorial region at 5, 4, and $3R_J$, and a continuous series of measurements (12 data samples) were obtained from 2.4 to $1.25R_J$. On the basis of pre-entry trajectory information, the spatial resolution of the data is $\sim 0.1R_J$ in the innermost region before the probe entered into the atmosphere.

H. M. Fischer, E. Pehlke, G. Wibberenz, Institut für Kernphysik, Universität Kiel, D-24118 Kiel, Germany.
L. J. Lanzerotti, Bell Laboratories, Lucent Technologies, Murray Hill, NJ 07974, USA.
J. D. Mihalov, NASA Ames Research Center, Moffett Field, CA 94035, USA.

Three different energy range channels were allocated to both electrons and protons in order to provide a rough estimate of the energy spectral dependence of each species over the energy range measured (Table 1) (*4*). Because of the expected low statistics, counts of heavy particles were accumulated over longer time periods than for the electrons and the protons. In addition to spin-averaged measurements, angular-sectored data were obtained for electrons, protons, and alpha particles in certain energy ranges in order to determine directional anisotropies and particle pitch angle distributions. The angular data were determined with the use of (i) magnetic field measure-

Table 1. Energy sensitivity of EPI channels, showing energy ranges for particle species having traversed the probe's aft heat shield. The given values were derived for an 18° mean angle of inclination of the particles' incoming direction with respect to the telescope axis, which is accurate for an isotropic particle distribution (*15*). Single energy values correspond to the lower limit for the channel. Upper energy limits exceeding 1 GeV are not contained in this table. Missing entries indicate no significant response to that species in that channel.

Channel	Energy ranges (MeV nucleon^{-1}) for particle species				
	e$^-$	p$^+$	He	C	S
E1	3.2	42	42	75	125
E2	8	62	62	110	210
E3	8	62	62	110	210
P1	66	42–131	42	75	125
P2	100	62–131	62	110	210
P3	203	62–92	62–530	110	210
He	450	–	62–136	110	210
HV	–	–	–	110–168	210